



# Experimental Investigation on the Effect of Increasing the Collar Thickness on the Flow Pattern around the Oblong Pier in 180° Sharp Bend with Balanced Bed

M. Moghanloo<sup>1</sup>, M. Vaghefi<sup>2, †</sup> and M. Ghodsian<sup>3</sup>

<sup>1</sup> Department of Civil Engineering, Persian Gulf University, Shahid Mahini St., Bushehr, 7516913817, Iran

<sup>2</sup> Department of Civil Engineering, Faculty of Engineering, Persian Gulf University, Bushehr 7516913798, Iran

<sup>3</sup> Faculty of Civil and Environmental Engineering, Tarbiat Modares University, Tehran, Iran

†Corresponding Author Email: [vaghefi@pgu.ac.ir](mailto:vaghefi@pgu.ac.ir)

(Received February 16, 2019; accepted May 12, 2019)

## ABSTRACT

In this paper, the effect of increase collar thickness has been investigated by considering other parameters affecting the flow pattern around the oblong bridge pier located at 90° from the 180° bend constant. Data acquisition was performed using the Vectrino 3D velocimeter. The leveling of the collar in both tests is constant and 0.4 times the pier diameter above the initial bed surface. The flow conditions were close to the motion threshold and bed balanced. The results showed that with an increase in the thickness of the collar by a factor of 4, the barrier surface is located in the flow path and the flow is deviated to the bed by colliding with the edge of the collar. This flow deviation that was due to the increase the collar thickness, led to 30% increase in the maximum depth of the scour hole upstream of the pier. Also, with the increase in the thickness of the collar, the tendency of the streamlines upstream of the pier to the inner bank increased, resulting in a 20% increase in the maximum sedimentation near the inner bank. The maximum turbulent kinetic energy at 80 degrees of the bend, corresponds with a protected pier with 3 mm thickness, equal to 620 cm<sup>2</sup>/s<sup>2</sup>.gr, which is reduced by 60% with increasing collar thickness.

**Keywords:** 180° sharp bend; Bridge pier; Collar; Flow pattern; Collar thickness; Kinetic energy.

## NOMENCLATURE

B	channel width	TKE	turbulent kinetic energy
b	wide of pier	UC	flow velocity under incipient motion conditions
d <sub>50</sub>	the average diameter of sediment particles	U	flow velocity
L	length of pier	y	upstream flow depth
PCT3	pier with a collar of 3mm Thickness	z	distance from the bed
PCT12	pier with a collar of 12mm Thickness	τ	Reynolds stresses
R	central Radius of the Bend		

## 1. INTRODUCTION

River bend paths are utmost importance in studying the flow pattern. The dominant pattern for the shape of the rivers in a natural systems is meander plan. The structure of meandering rivers is more complex than straight flow rivers. The main force applied on the flow in bends is centrifugal force, which causes the formation of secondary flow. Due to the interaction between secondary currents and lack of

uniformity of velocity profile in depth due to the shear stress on the bed, a flow pattern called the spiral flow is formed along the channel. This spiral flow plays a main role in the formation and development of bed changes and also the distribution of shear stress at the channel's bottom. The existence of structures such as in-bend bridge piers affects on spiral flow pattern in the bend and increases the complexity of flow behavior.

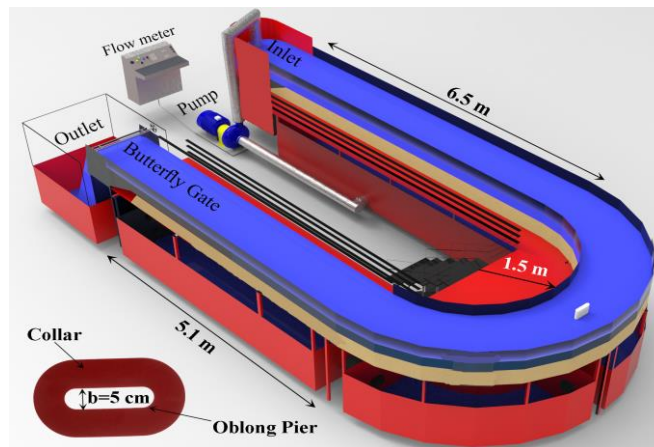


**Fig. 1. Channel plan and laboratory setup.**

Furthermore, locating the pier on the flow makes a change in it. So, it creates vortices that are known as the main reason of scouring around the bridge pier. The horseshoe vortices at the upstream of the pier and the uplift vortices downstream the pier are important factors for scouring around the bridge piers. Therefore, understanding the flow pattern around the pier and on the condition of locating the pier on the bend is highly important. In the meantime, the existence of collar adjoining structure used for reducing scour around the pier increases this complexity (Abdi Chooplou and Vaghefi, 2019). Many researchers from the past so far have been trying to study the structure of the flow around the bridge piers with numerical and experimental methods. These include Dey and Raikar (2007), Kirkil *et al.* (2008), Rodriguez and Garcia (2008), Belcher and Fox (2009), Beheshti and Ataie-Ashtiani (2010), Kirkil and Constantinescu (2010), Şarлак and Tiğrek (2011), Kumar *et al.* (2012), Ataie-Ashtiani and Aslani-Kordkandi (2012, 2013), Das *et al.* (2013a, 2013b), Das and Mazumdar (2015), Ma *et al.* (2015), Beheshti and Ataie-Ashtiani (2016), Tryggvason *et al.* (2016), Ma *et al.* (2016), Karimi *et al.* (2017), Khan *et al.* (2017) in the straight path and also Naji Abhari *et al.* (2010), Barbhuiya and Talukdar (2010), Constantinescu *et al.* (2011), Uddin and Rahman (2012), Tang and Knight (2014), Vaghefi *et al.* (2015), Vaghefi *et al.* (2016), Ben Mohammad Khajeh *et al.* (2017), Dey *et al.* (2017), Vaghefi *et al.* (2017), Abdi Chooplou *et al.* (2018), Gholami *et al.* (2019) in the bend. Considering that previous studies have shown that there was no comprehensive study on flow pattern around the bridge pier with collar in the case of placement in bend, it is important to understand the pattern of the flow around the bridge pier protected by collar. Important parameters in the case of adjoining structure of collar affect the flow pattern and thus the scouring process around the combination pier and collar (Zarrati *et al.*, 2004). One of these parameters is the thickness of collar. In the present study, the effect of increased collar thickness on the flow pattern around the oblong bridge pier located in the 180° bend has been investigated. The three-dimensional flow pattern surrounding the composite

structure and its details are of the issues discussed in this paper.

## 2. MATERIALS AND METHODS

The experiments were carried out in a channel with an 180° bend at the Hydraulic Lab of Bushehr University of Persian Gulf. Figure 1 shows the plan and geometry of the bend. This channel includes a straight path of 6.5 meters in the upstream, and also a straight path of 1.5 meters in the downstream, which have been connected by an 180° bend with central curvature radius of 2 meters. The channel is made of glass, whose stability is maintained by steel frames. The ratio of the bend radius to the channel width is 2 and its height is 70 cm and the width is 100 cm. considering that the ratio  $R/B = 2$  ( $R$  is the center radius,  $B$  is the channel width), according to the classification by leschziner & Rodi (1979), this bend is in the category of sharp bends. The bottom of the channel up to 30 cm includes sediments with an average diameter of 1.5 mm and a standard deviation of 1.14. The discharge rate was adjusted by an ultrasonic flowmeter of AKTEK (TFM3100-F1) by the accuracy  $\pm 1\text{mm/s}$  installed on the inlet pipe. A butterfly gate was used at the end of the channel to control the flow. All experiments have been carried out in conditions close to the motion threshold with the flow velocity to critical velocity ratio of ( $U / U_c$ ) of 0.98. According to Oliveto & Hager (2002) to prevent the effects of roughness, the depth of water should be higher than 20 mm, so the discharge was 70 liters per second and the water depth was 17.8 cm for tests.

Scouring was measured after the relative equilibrium time. To this end, the channel bed was meshing. This mesh was non-uniformly and around the pier were smaller. To measure the altered topography, a laser device with the accuracy of  $\pm 1\text{mm}$  was utilized. To stabilize and rigidify the bed changes caused by scouring experiments and after the bed reaches the relative equilibrium, concrete adhesive, air compressor and fiberglass adhesive were used to measure the three-dimensional flow rate. Three-dimensional Vectrino velocimeter has been used to measure the velocity

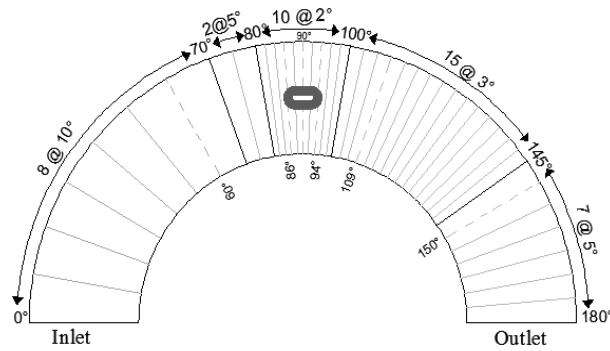


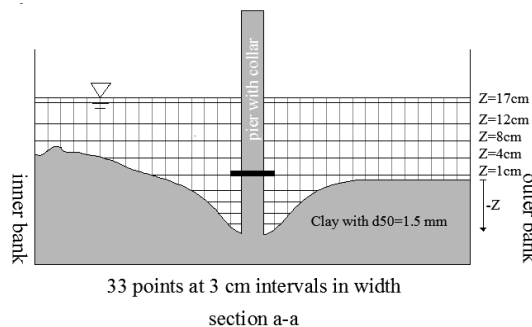
**Fig. 2. View of the mesh along the channel.**

components and determine the three-dimensional flow pattern. The maximum sample frequency of the device was 200 Hz that can be regulated by the software from 1 Hz to 200 Hz. The velocity can be regulated, by the user, from 0.01 to 7 m/s with the accuracy  $\pm 1$  mm/s.

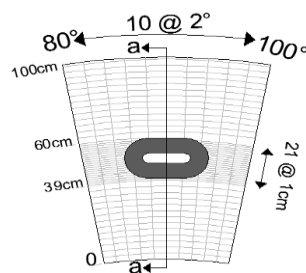
The mesh used in this study to measure the velocity components in the range 0 to 180° in 42 longitudinal sections and 33 points in each section at 3 cm intervals (Fig. 2).

side-looking probe in Fig. 4. Also at least 4 levels lower than the initial bed have been measured in the scouring holes. The velocity recorded time for each node of the mesh was 1 min. The same time, 1 min, was spent for regulating the device on each node, considering the number of nodes that shown in Figs. 2 and 3 the data was collected approximately 20 work days.

Two tests of scour and flow patterns were performed by installing the collar with different thicknesses around the oblong pier. Also, according to [Melville & Sutherland \(1988\)](#), the length of the rectangular pier should be at least 3 times its width. Therefore, for the experiments, a pier with a width of 5 and a length of 20 cm ( $L/b = 4$ ) was used with rounded upstream and downstream nose. First, in the first experiment, a collar with thickness of 3 mm was placed around the pier (PCT3), this thickness in the second experiment was 4 times (PCT12), and the effect of the collar thickness on the flow pattern has been investigated. The width of the collar is 4 times the width of the pier, which was installed at the level of 0.4 times the pier width, equivalent to 2 cm above the bed surface at the beginning of the bend around the pier. The collar and the pier used are respectively made of plexi-glass and PVC. Figures 4(a) and (b) respectively indicate the receiver tentacles in the down-looking mode and the receiver tentacles in the side-looking mode of the three-dimensional vectrino velocimeter. Also, in Figs.4(c) and (d), a side-looking probe is used to measure the velocity near the water surface and, if possible, below the collar.



(a)



(b)

**Fig. 3. View of the mesh in a) channel width b) around the pier at section a-a.**

This mesh around the pier has been segmented to 2 degrees in length and 1 cm in width, as shown in Fig. 3(b). According to Fig. 3(a), the mesh was measured at 5 levels above the initial bed that the levels of 1, 4, and 8 cm have been shown with down-looking probe and 12 and 17 cm levels by

### 3. RESULTS AND DISCUSSION

Figure 5 shows the bed topography in scouring patterns after relative equilibrium. As it is evident, a scouring hole has been created near the inner bank of sedimentation and around and below the pier. The maximum scour depth in the test (PCT3) and (PCT12) is respectively 2.24 and 2.78 times the pier diameter near the pier. The sedimentation has been created for both experiments in the range of 30% of the channel width from the inner bank from the angle of 20 to 150 degrees of bend, the maximum of which for tests (PCT3) and (PCT12) was 1.7 and 2 times the measured pier diameter.

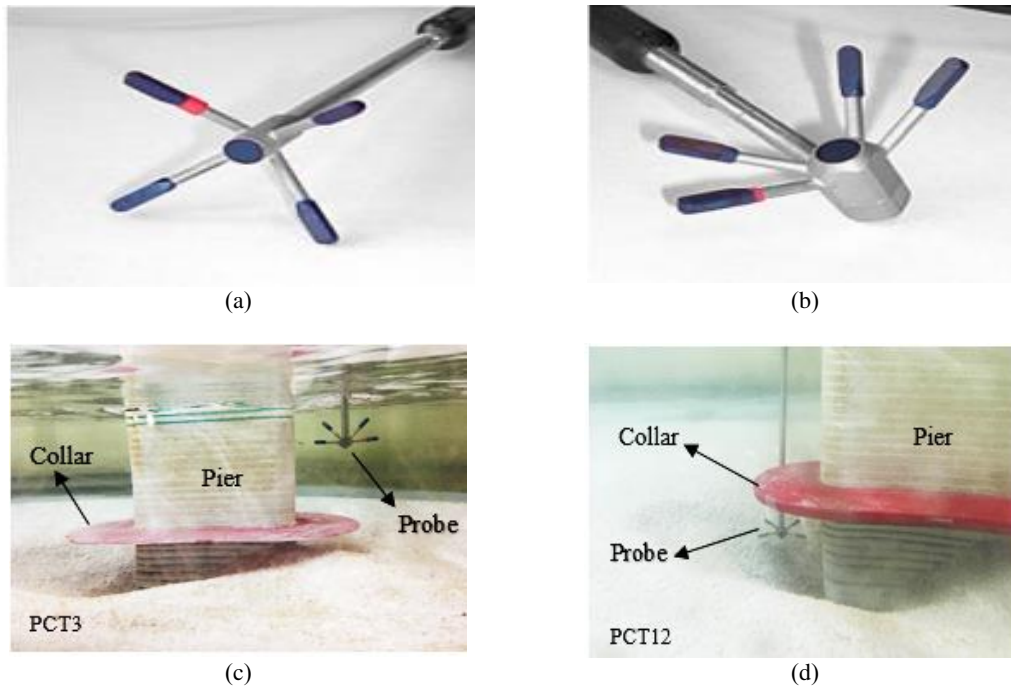


**Fig. 4.** Presentation of the a) down-looking b) side-looking probe and a view of the velocity measuring c) Near the flow surface d) Below the collar.

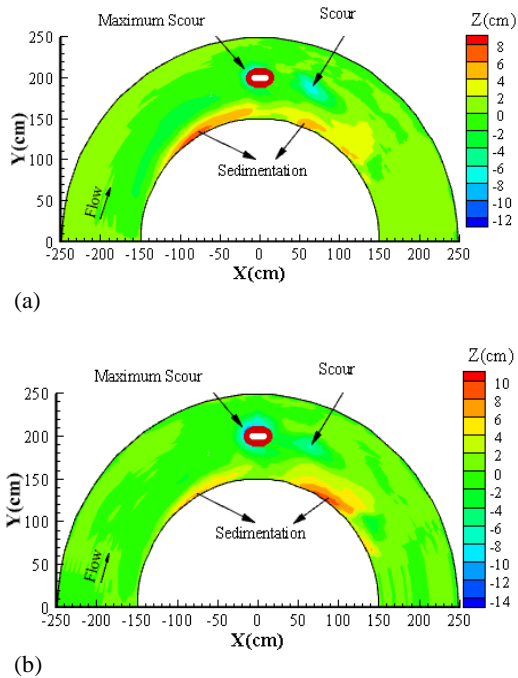


**Fig. 5.** Bed topographic changes in flow pattern experiments a) Oblong pier with 3 mm collar thickness (PCT3) and b) Oblong pier with 12 mm collar thickness (PCT12).

In Fig. 6, an example of streamlines in the lateral sections 60, 86 degrees of bend and at the pier upstream and collar have been presented in both experiments. In the aforementioned figure, the secondary flow is clearly observed. The secondary flows, due to the rotational properties of the flow in

lateral sections, cause lateral transfer of the longitudinal momentum of the flow and the increase in shear stress applied to the floor and the sides of the bend. The longitudinal pressure gradient due to the change in the water level along the inner and outer walls of the bend can lead to the transfer of high-velocity flow to the inner and outer bank. The interaction of the abovementioned factors (secondary flow, longitudinal pressure gradient) and factors such as bend geometry, flow characteristics, sedimentation of bed and pier of the bridge along with the collar placed in the path of the flow leads to applied shear stresses with different distributions near the bed and the bend walls.

In Fig. 6(a), the flow pattern in the upstream of the pier location to the angle of 60° equivalent to 20 times the pier diameter is similar for both experiments, indicating that at this stage, the change in the thickness of the collar has a small effect on the flow pattern and ultimately the bed topography changes. Near the inner and outer banks, vertical velocities are dominant over the radial velocities which is due to the collision of flow to the bend walls. The rotational flow center in both tests is about 30% of the channel width from the inner bank, which can be attributed to the maximum scour depth at this position.

Figure 6(b) shows the streamlines in the lateral cross section at the upstream edge of the collar. As the curve progresses along the bend, the effect of the curve radius of the bend with the inclining of the streamlines in the outer half of the bend extends to the floor of the bed. At this section, in both experiments, two rotational flows with a radius of approximately 2 times the pier diameter at 30% of the channel width from the inner bank have been

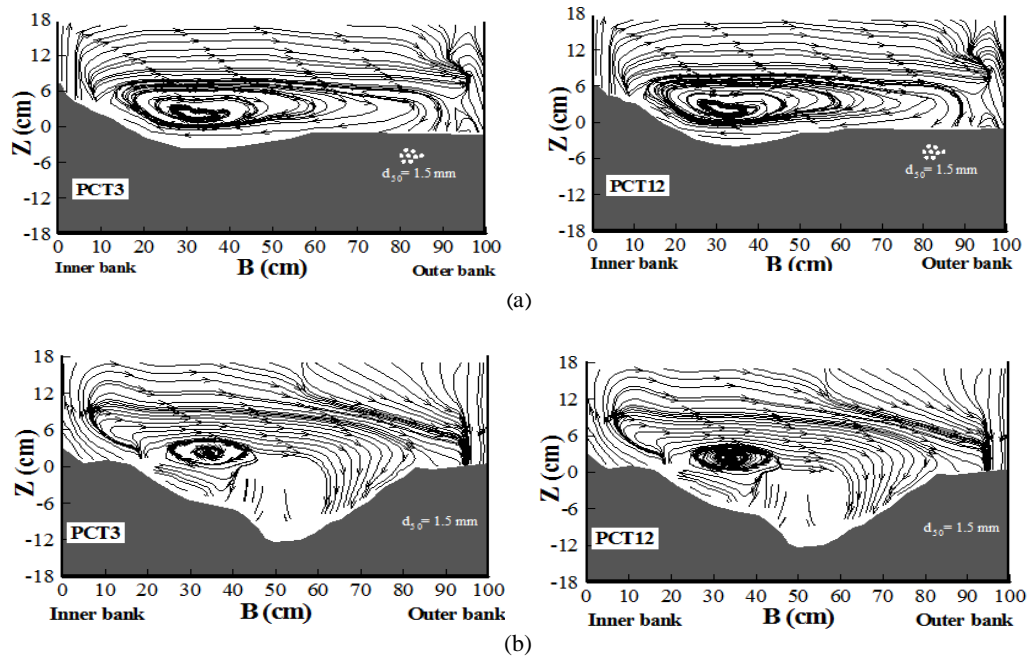


**Fig. 6.** Streamlines in the lateral sections on the upstream of the pier a) 60 and b) 86° of bend.

formed. According to the figure, it is observed that the collar prevents the complete formation of this rotational flow and prevents the collision of downward flows to the bed caused by collision with the pier.

By comparing the topographic changes of the two experiments, it can be concluded that in the PCT12 test, the deviation of the lines in this region toward the bottom of the bed is greater due to the presence of a higher surface area of the collar thickness against the flow compared to the PCT3 test. Also, near the outer bank, the imperfect second secondary flow is observed.

An example of the streamlines in the lateral sections from the vertex to the end of the bend for both experiments has been shown in Fig. 7. Figure 7(a) shows the lateral cross section in the pier position. As observed, the presence of pier with collar connected to it causes the separation of flow in this region and creates two rotational flows on the sides of the pier. The flow deviates to the bed by colliding the pier.

According to this figure, in the PCT12 test, by increasing the collar thickness and deepening of the scour hole on the sides of the pier, two rotational flows have been formed, the center of one of which is in the outer half of the bend at the distance of 40% of the channel width from the outer bank under the collar, and the other in the inner half of the bend at the distance of 30% of the channel width from the inner bank at the collar level. On the inner half of the bend, the streamlines under the collar move toward the inner bank in upward manner after collision. These streamlines transfer some of the scouring sediments during the time of equilibrium to the inner bank and place some other in the direction of the longitudinal flow that moves

towards the bend outlet. Thus, simultaneous collar and pier transform the secondary flow formed in the bend into two secondary flows. The same pattern is observed in the PCT3 test, but because of the smaller scour hole, the location of the center of the vortices has changed.

Downstream the pier at the lateral section of 94 degrees, the bend of the equivalent bend with the position of the downstream edge of the collar, as shown in Fig. 7(b), on the collar, the vertical velocity has been dominant over the radial velocity, causing uplift flow. This uplift flow in the PCT3 and PCT12 tests is observed at the height of 30% and 50% of the flow depth from the water surface, which is the location of the separation of the two secondary clockwise flows formed at this point. Figure 7(c) shows the lateral cross section at the location of maximum depth of the scour hole on the downstream of the protected pier. Moving downwards and taking distances from the pier location gradually decreases the impact of the pier protected by the collar on streamlines. Considering that in the PCT3 test near the bed surface, the scouring hole of the streamlines does not have a regular pattern, but there is a counterclockwise rotational flow near the flow surface in the middle of the channel. In the PCT12 test, streamlines at a distance of about 50% of the flow depth from the water surface are downward inclined towards the outer bank. Also, in this experiment, two rotational flows are spaced at 30% of the channel width, one in the place of the scouring hole and the other in the other half of the bend. Figure 7(d) shows the lateral cross section at the angle of 150°, equal to 2 times the channel width at the downstream of the protected pier position. At this section, in both experiments, in the outer half of bend, the direction of streamlines at 30% of the flow depth is from the

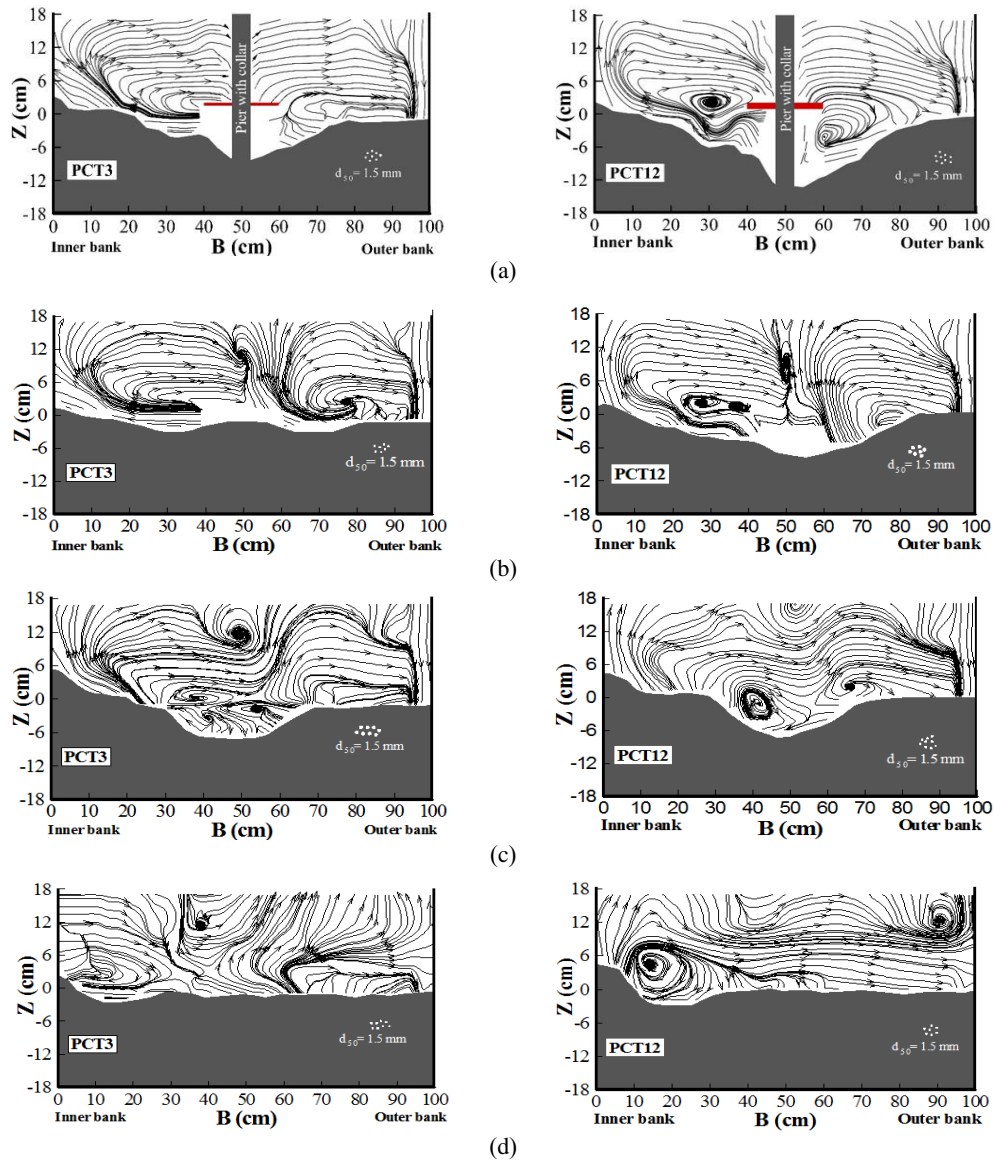
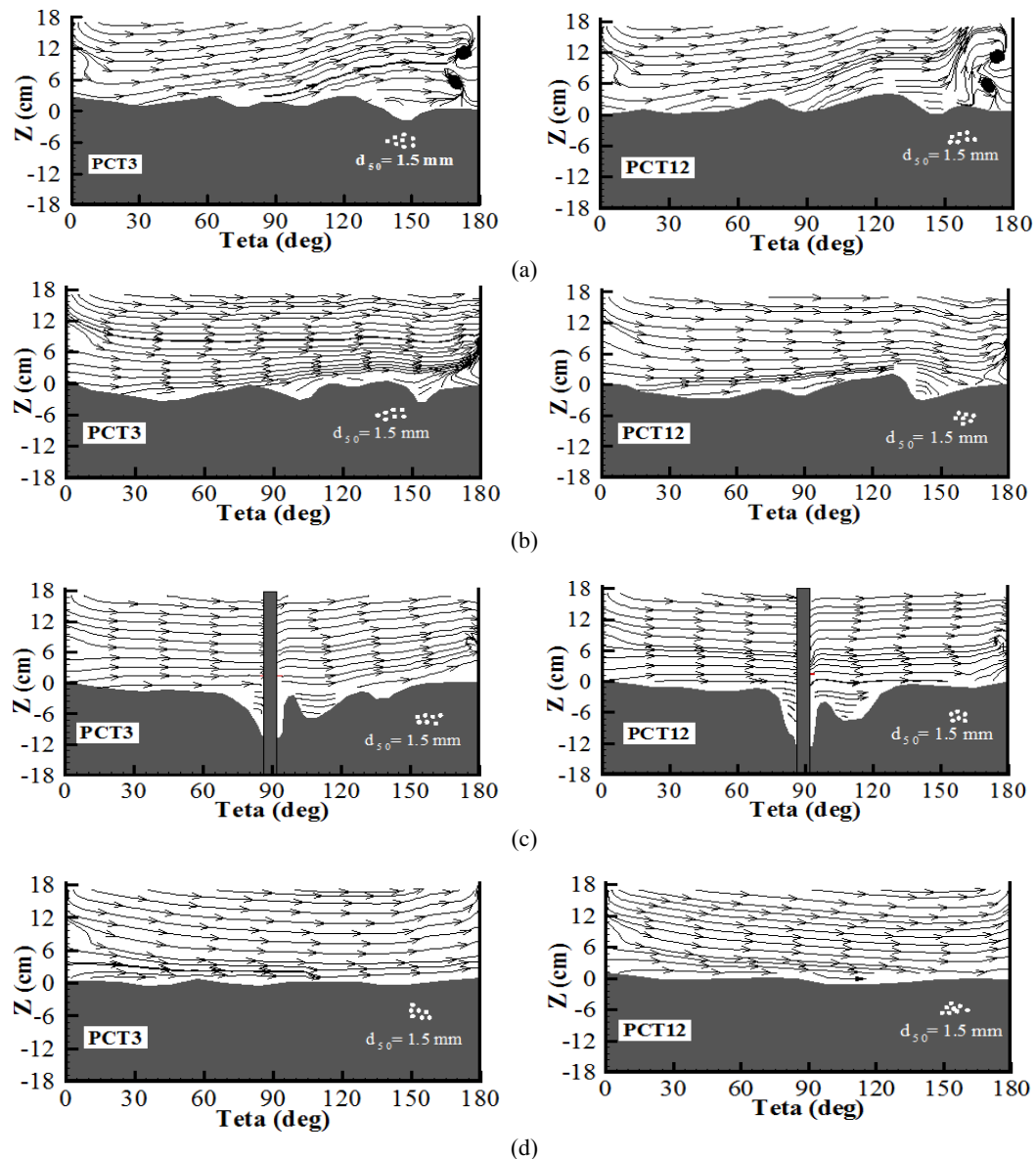


Fig. 7. Streamlines in lateral cross sections a) 90, b) 94, c) 109 and d) 150° of the bend.

bed surface to the outer bank. While the pier upstream at the angle of 60° of the bend (Fig. 6(a)), the direction of the streamlines in this region is reverse. In the vicinity of the inner bank, there are two rotational holes in the scour hole. In the PCT12 test, the rotational flow center is at the distance of 15% of the channel width of the inner bank and 30% of the flow depth from the initial bed surface. In the PCT3 test, a rotational flow with a distance of 35% of the channel width from the inner bank and 30% of the flow depth from the flow level has been formed. Also, at this section, the second secondary flow is again formed near the water surface and on the outer bank with a counterclockwise direction formed, which is more evident in the PCT12 test.

Figure 8 have presented examples of streamlines in longitudinal sections at different distances from the channel width for both experiments. As shown in Fig. 8(a), there is a downward flow at the distance of 5% of the channel width from the inner bank and

70% of the flow depth from the water surface at the channel inlet. In most of the distances at this section, this trend is reverse and the flow direction is upward, which can be due to the collision of flow with stacks deposited in this area and after the balance of the bed. In fact, the vertical velocity has increased in this area. This causes the formation upward flow and return flow at the water surface. Also, in both experiments, in the output of the bend, two rotational flows have been formed at the distance equal to the pier diameter on each other. Figure 8(b) shows the longitudinal section at a distance of 25% of the channel width from the inner bank in each of the two experiments. At this section, considering that the sedimentation rate is less than that of the inner bank, the rate of deviation of the streamlines near the bed also decreases. In this region near the bed surface due to the bed topography changes of the streamlines has been deviating. Figure 8(c) shows the longitudinal



**Fig. 8.** An example of the streamlines at different longitudinal sections of 180° at a distance equal to a) 5, b) 25, c) 50, and d) 95 percent of the channel width from the inner bank.

section in the center line of the bend equivalent to 50% of the channel's width from the inner bank. In this figure it is observed that, the flow pattern is affected by the presence of a protected pier. It is worth noting that in the area surrounding the protected pier due to the geometry of the scour hole and the velometer limitation, it was not possible to measure the velocity in some places. As seen in Fig. 8(c), with collision of flow with the pier, the downward flow is formed on the pier upstream and at a level above the initial level near the initial bed. In fact, the presence of the collar around the pier prevents the collision of downstream flow to the bed bottom and greatly reduces the scouring resulting from this flow. On the other hand, considering that the collar has been placed at a level above the initial surface of the bed, the flow penetrates below the collar, and a downward flow with strength lower than the downward flow of the

case without collar is formed. Since collar in both tests have been installed at an identical level, the tendency of the streamlines in the pier protected with collar with higher thickness (PCT12) to the bottom of the bed is higher due to the greater depth of the scouring hole. At the downstream of the pier, the vertical velocity is upward, which causes uplift flow after the flow passing from the pier. Streamlines at the distance equal to 10 times the pier diameter at the downstream of the protected pier near the bed are upward, due to the collision with the downstream wall of the scour hole. By approaching the outer bank, due to low variation of the bed topography, the streamlines of the flow become more uniform. While, within 5% of the channel width from the outer bank to 60% of the flow depth from the water surface, streamlines have been parallel and aligned with each other and are inclined toward the flow surface in bend outlet

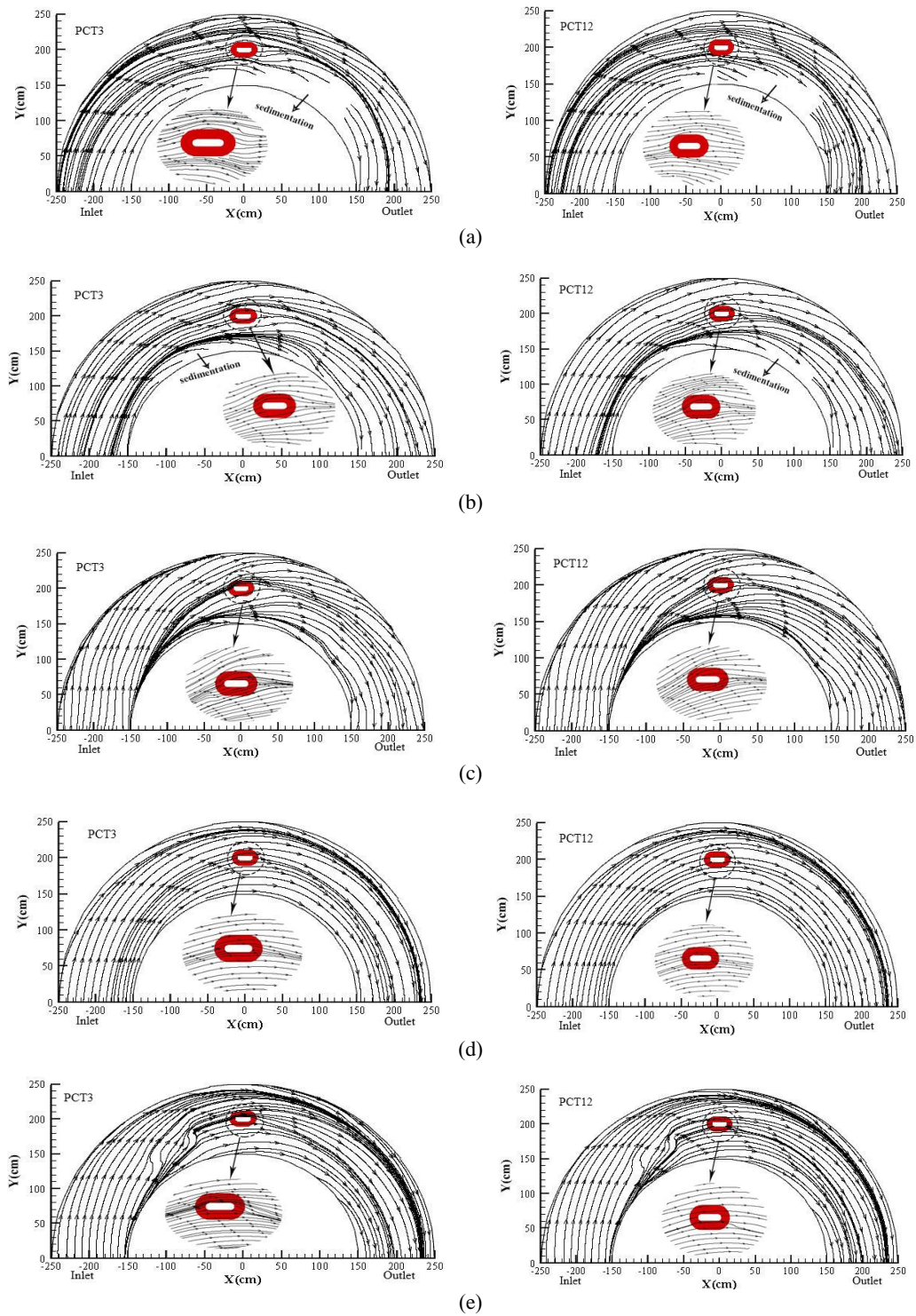


**Fig. 9.** Streamlines at the levels of a) 5, b) 20 and c) 45 percent of the flow depth at the beginning of the bend from the bed bottom; and d) 35 and e) 5 percent of the flow depth at the beginning of the bend from the flow surface.

which indicates the existence and formation of the second secondary flow in the end of bend (Fig. 8(d)).

Figure 9 represents the streamlines in the plan for both tests (PCT3) and (PCT12). In order to better illustrate the pattern of flow around the pier,

magnification of the streamlines around the pier is also given. Figure 9(a) shows the streamlines at 1 cm above the bed. As observed, in the first half of the bend associated with both experiments, due to the friction of the flow at the bed bottom, the flow force dominates the centrifugal force and the flow direction inclines towards the inner bank. The



**Fig. 10. Flow pattern around the pier a) View of the inner bank and b) Pier nose.**

inclination of the flow towards the inner bank transfer suspended sediments near the bed surface to the inner bank, resulting in the formation of sedimentary stacks on the inner bank of the bend. For this reason, velocity at levels in the range of sediment stack heights in these areas is zero. As seen in the magnified figure, streamlines are separated from each other by the collision of flow to the pier, the direction of which is towards the outer half of the bend to the outer bank and the outer half of the bend toward the inner bank. Considering the geometry of the bend, the movement of these lines toward the outer bank has led to scouring near the outer bank. It should be noted that at the pier upstream below the collar at the distance between these separated streamlines, the streamline collides with the pier with the collar and transforms to the downward flow, which results in the formation of a scour hole in the pier nose. The deviation of the streamlines in the PCT12 test is also higher due to the higher collar thickness. The movement of this downward flow leads to the suspension of scour hole sediment, and as the flow inclination in this area is more towards the inner bank, the sediments of this scour is moved to the inner bank and the height of the sedimentary stacks has increased. On the other hand, the streamlines at the downstream of the pier separated from each other by the collision with the pier, are connected at the center line of the bend. The connection location of these streamlines separated from each other in the PCT3 test from the pier tail is 12 times the pier diameter, which increased by 60%. At the outlet of the bend in both tests, the flow inclination at this level is toward the middle of the channel.

In Fig. 9(b), the streamlines at 4 cm above the bed surface have been shown in both experiments. Due to the fact that the collar has been installed at the level of 2 cm above the bed surface around the pier, so in this figure the streamlines pass through the collar. At this level, the streamlines in the first half of the bend in the PCT3 test are inclined to the inner bank, that, these lines are approximately parallel to the central line of the channel as the thickness of collar increases. On the other hand, sedimentation near the inner bank of this area causes irregularities in the streamlines. The flow velocity decreases with collisions with sedimentary stacks at this level. Considering the magnification of the figure, the collision of the flow to the pier causes the divergence of the flow at the pier downstream and

causes the flows in the outer half moving toward the downstream inclines towards the outer bank. Also, the connection location of these lines separated from each other at this level in the PCT3 test did not change much compared to the previous level (Fig. 9), but in the figure associated with the PCT12 test, the separation location of lines were reduced by 4% compared to the previous level. Figure 9(c) shows that the streamlines at 8 cm above the bed surface for both tests at the beginning of the bend are parallel with the straight upstream path. According to the figure, it is observed that these lines at  $50^\circ$  of the bend are divided to three groups of moderate, inclined to the inner bank, inclined to to the outer bank. At this angle, 80% of the channel width from the outer bank is related to the lines inclined to the outer wall of the bend. The moderate lines have a high density which are directed to the outer bank by colliding to the pier on downstream. In the magnification of the figure of the PCT3 test, it is observed that the moderate lines of the inner half of the bend at the distance of 2 times the pier diameter at the pier upstream are inclined to the inner bank. But, with an increase in the thickness of the collar, these lines are deviated by collision with the pier. The separated lines in both experiment are connected at the distance of 10 times the pier diameter at the downstream of the pier. As shown in Fig. 9(d), it is observed that the streamlines in the first half of the bend are uniform. At this level, the divergence of the flow with the collision with the pier is lower and the flow is transferred to downstream with regular pattern. Figure 9(e) shows the streamlines at 1 cm below the flow surface. It is observed that the increase in the thickness of the collar at this level does not have much effect on the flow pattern. As it is evident, the flow with the regular pattern entered into the bend and due to the fact that the centrifugal force near the water surface prevails over other forces, the average deviation of the streamlines is towards the outer bank. This increases the depth of flow on the outer bank. The collision of flow with the pier cause a return flow on the pier upstream and increases the flow depth in the pier nose. Clearly, this increase in the flow depth is qualitatively seen in Fig. 10. The return flow also causes the deviation of the flow to the outer bank of the bend. Considering the inclination of flow to outer bank of the bend and decrease in the section width at the pier location, the flow velocity in this range increases.

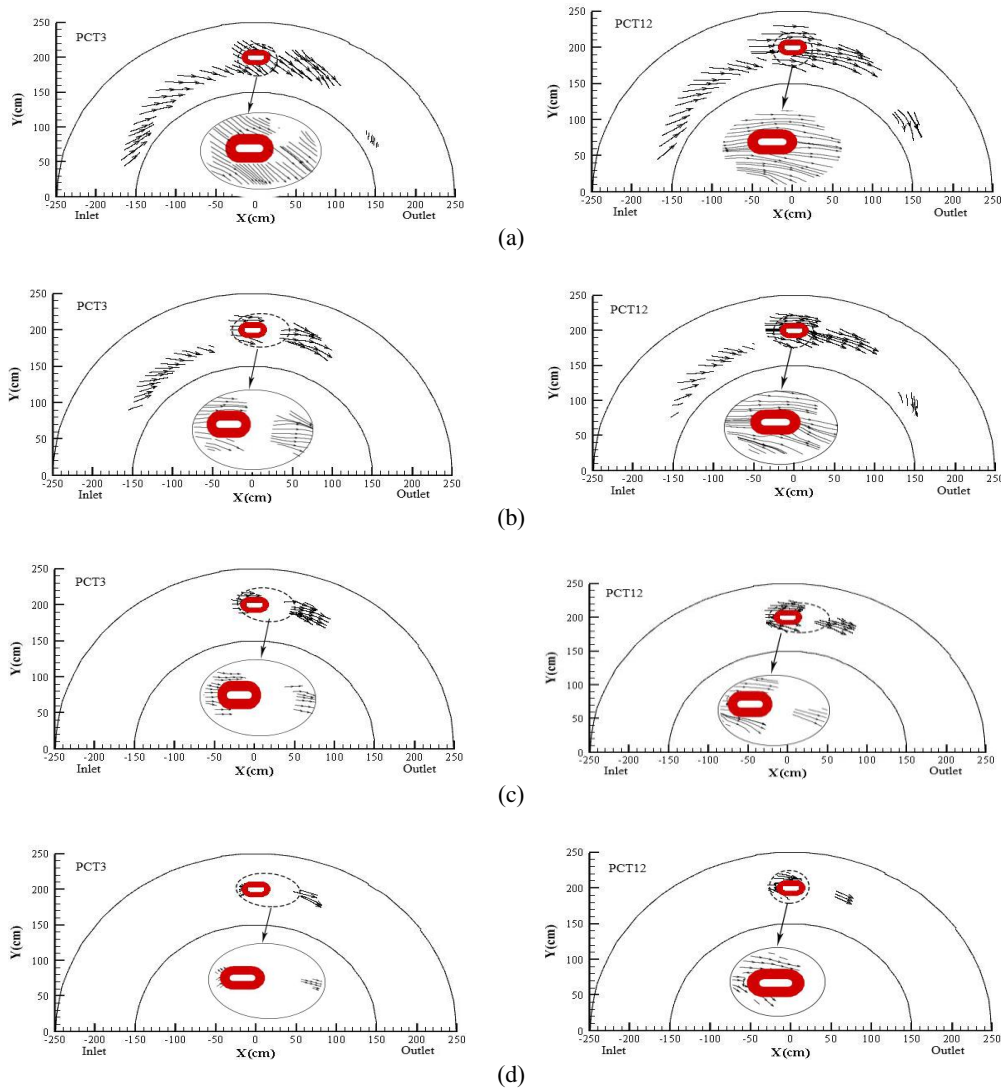


**Fig. 11. Streamlines at the levels of a) 5, b) 10, c) 20 and d) 30 percent of the flow depth at the beginning of the bend, lower than the initial bed.**

Figures 11(a) and (b) show streamlines in the lower levels of the initial bed in both experiments. As it is evident, the radial velocities in these equations are negative, with tangential velocities approaching the inner bank. As a result, suspended sediments in the scour hole are driven to the inner bank. The magnification of the images related to the PCT3 test shows that on the downstream of the pier, due to the lower scour depth compared to the PCT12 test, the flow does not completely pass below the collar and collides the inclined hole of the scour hole. But by increasing the thickness of the collar, the flow deviates toward the bed due to collision with collar edge which increases the depth of the scour hole around the pier. Also, in the scouring holes created in the second half of the bend, the flow direction inclines toward the inner bank in both tests. Figures 11(c) and (d) show the streamlines in both experiments at levels equal to 20% and 30% of the flow depth at the beginning of the bend lower than the bed bottom. The inclination of the streamlines at these levels is almost toward the inner bank. In the

magnification of the images it is seen that the flow changes after the collision to the pier under the collar. As the collar thickness is increased, the angle of deviation of the streamlines in the inner half of the bend at the collision point to the pier is higher than the outer half of the bend and the PCT3 test. Comparing the lower levels of the bed in the range of scour holes with the upper levels of the bed, it can be said that the inclination of the streamlines at all lower levels of the bed is towards the inner bank.

Figure 12 shows the geometric location of the maximum velocity in the bend at the levels of 5, 45, 95% of the flow depth from the bed surface in both experiments. In all figures, at the beginning of the path bend, the maximum velocity is located near the inner bank.

Approaching the location of the pier, the geometric location of the maximum velocity has been separated from the inner wall and tends to the middle of the channel. With the collision of flow to the pier, the resultant of this velocity changes, as in

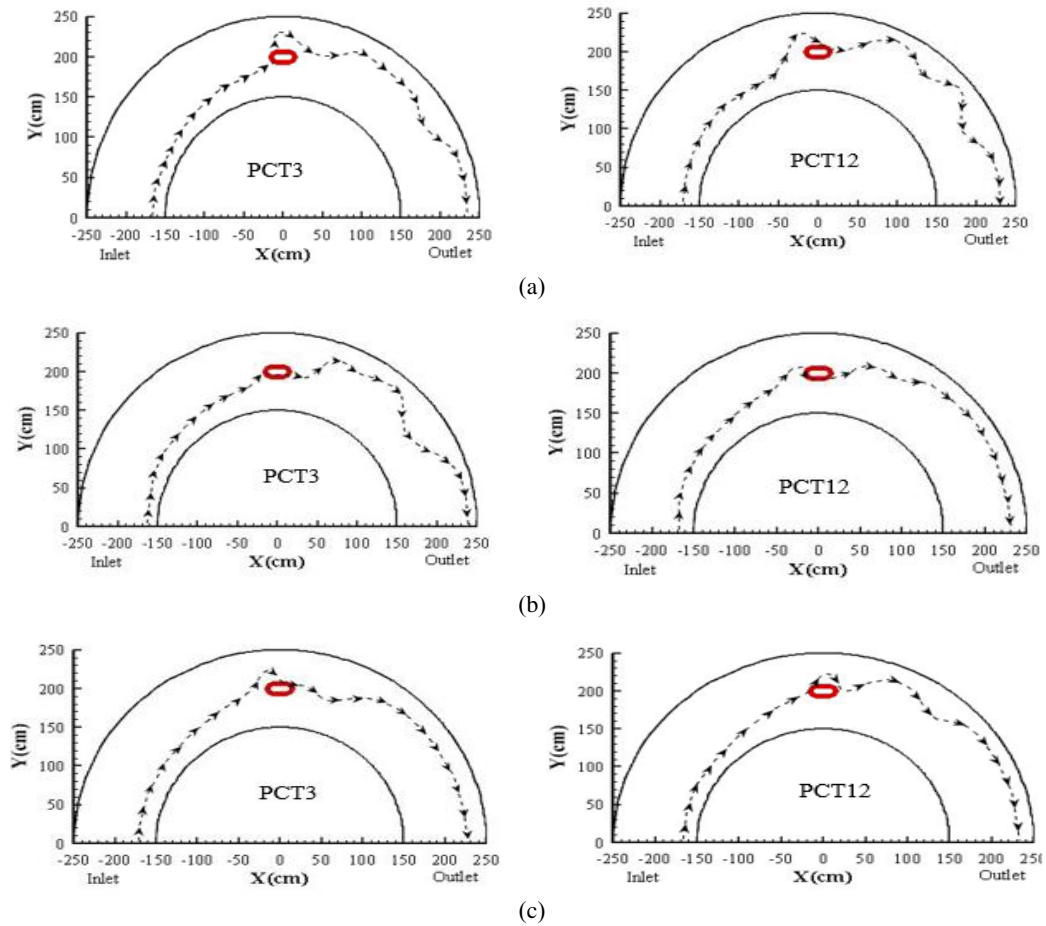


**Fig. 12.** Path of formation of the maximum velocity resultant at the levels of a) 5, b) 45 and c) 95% of the flow depth from the initial level of the bed surface.

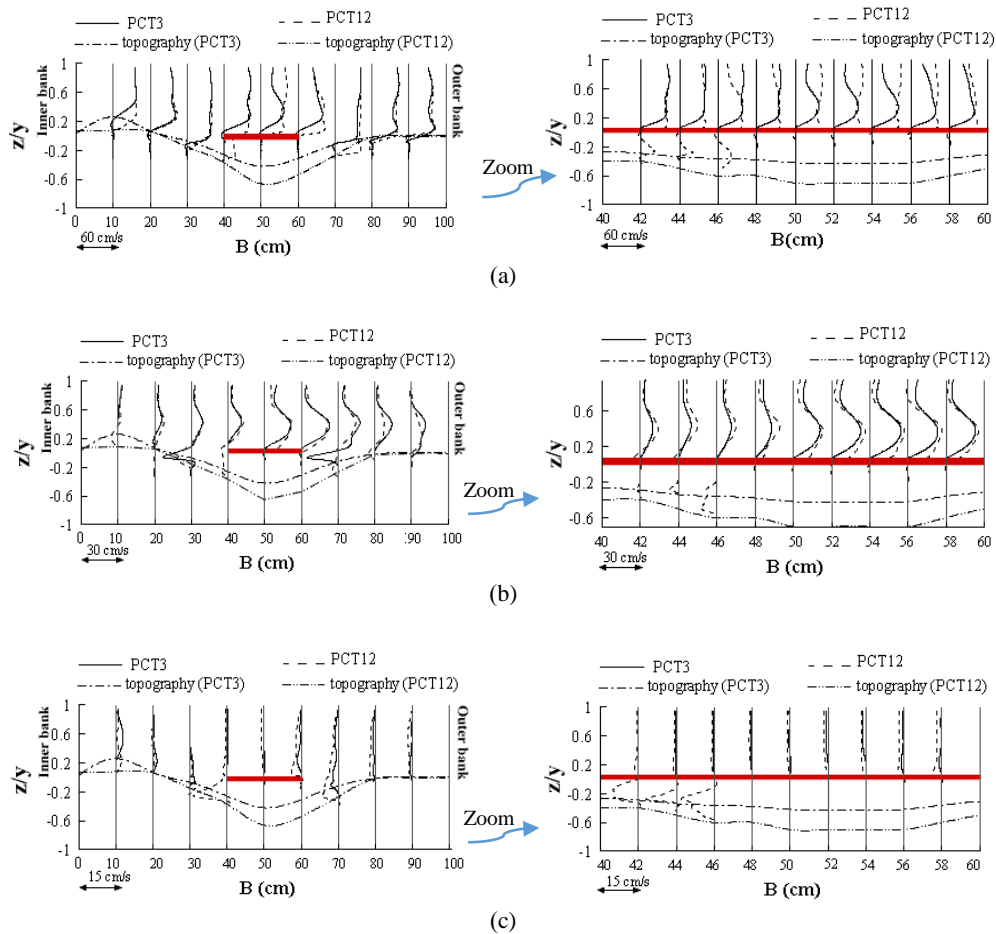
Fig. 12(a), in the PCT3 test, it moves from the upstream pier to the outer bank and takes distance from the pier, but with the increase in the thickness of the collar (PCT12), this maximum consequent approaches to the pier. In Fig. 12(b), at the level of 45%, the depth of flow at the beginning of the bend from the initial bed surface in both the collar thicknesses, the geometric location of the maximum velocity passes the collar face which is near the inner bank of the bend, and then, according to the topography of the bed toward the outer bank, they pass with a little difference relative to each other. But at 95% of the flow depth at the beginning of the bend from the initial bed surface (Fig. 12(c)), this path passes from the face close to the outer bank of the collar and inclines toward the outer bank in the second half of the bend. As can be seen, the effect of increasing the collar thickness on the geometric location of the maximum velocity decreases by approaching the flow surface. Generally, at all levels, the maximum velocity resultant has been formed at the bend outlet at the distance of 5% from the outer bank.

Figure 13 represents the changes in tangential, radial and vertical velocities at a cross-section of 86 degrees from the bend. The magnitude of figure in the width of the collar is also given to examine the

effect of increasing the thickness of the collar on the velocity values.

Figure 13(a) shows the changes in tangential velocity. As it can be seen, sedimentary stack is formed in the distance of 10% of the inner bank in the PCT3 test, which increasing the collar thickness prevents the sedimentation in this area. Therefore, in the PCT12 test in this area, the flow has a positive tangential velocity (downward). At the upper edge of the collar, the tangential velocity increases as the collar thickness increases. On the other hand, in the distance of 30% of the outer bank, the values of tangential velocity in both tests are close to each other and are downward. Figure 13(b) shows the radial velocity changes in the channel width.

The angles of the curves of this graph with the vertical axis indicate the existence of transverse vortices at these points. It can be seen that at 30% of the width of the channel from the inner bank in the range of the scour hole in both tests, the radial velocity is negative, which indicates the flow is toward the inner bank and as it approaches to the flow level, the direction is positive and toward the outer bank. This change in direction in the bed level indicates the presence of vortices in this area. Between 40 and 60% of the channel's width from



**Fig. 13. Velocity graph a) tangential, b) radial and c) vertical in a cross section at 86 degrees angle of bend.**

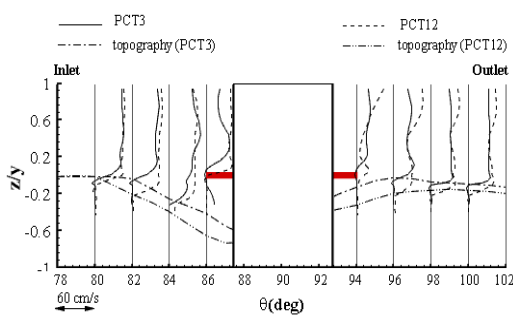
the inner bank is equal to the collar width of the positive radial velocity (toward the outer bank) and it escalates with increasing collar thickness. Also by magnifying this figure near the inner bank, the direction of radial velocity is negative and toward the inner bank, which can be seen easily in the PCT12 test. Figure 13(c) shows the changes of vertical velocity in the cross-section. According to this figure, at a distance of 30% of the channel's width from the inner bank, the vertical velocity is positive and towards the flow level and by approaching the pier position, and in the outer half of the bend, the direction of vertical velocity in both tests is negative and toward the bed. Considering the magnification of this figure above the collar level, vertical velocity is small, which can be due to clash of flow to the collar level, and also by increasing the collar thickness the tendency of flow is going toward the bed.

Figure 14 shows the distribution of tangential, radial and vertical velocities in a longitudinal section at a distance of 50% of the channel width from the inner bank in PCT3 and PCT12 tests. This longitudinal section indicates the velocity changes at different levels and at a distance of 7 times of the pier diameter above and below the protected pier is equal to the angle of 80 to 100 degrees of the bend.

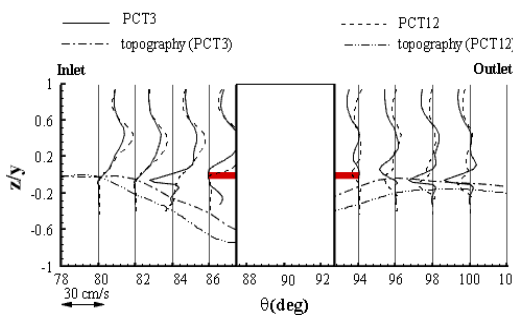
Horizontal axis of the graph in terms of degree and representing the bend position and in vertical axis,  $y$  is depth of water at the beginning of the bend. According to Fig. 14(a), at a distance of 7 times of the pier diameter above the protected pier, the tangential velocity in both tests is similar. By increasing the collar thickness, the scour rate in the pier nose increases by 30%. At an angle of  $86^\circ$  above the collar level at a distance of 70%, the flow depth from the water surface the tangential velocity in the PCT3 test decreases closer to the level of the collar, but with the increase in the collar thickness, the tangential velocity in this range is approximately the same and about 36 cm/s. At the bottom of the protected pier, the effect of increasing the collar thickness is more evident, so that at an angle of 94 degrees, the increase in the collar thickness the tangential velocity at the surface of the water increases by 10%. Also, at the bottom of the protected pier in the PCT3 test, the tangential velocity at a distance of 80% of the flow depth from the water surface is roughly the same, but with increasing the collar thickness, the tangential velocity decreases at this range. In Fig. 14(b), radial velocities have an irregular pattern. In the range shown in both tests, radial velocity values vary in different levels. In both tests near the surface of the water, radial velocity is positive and towards the

outer bank. By approaching the bed level, the radial velocity is reduced and the direction gets negative, indicating the flow of the current is towards the inner bank.

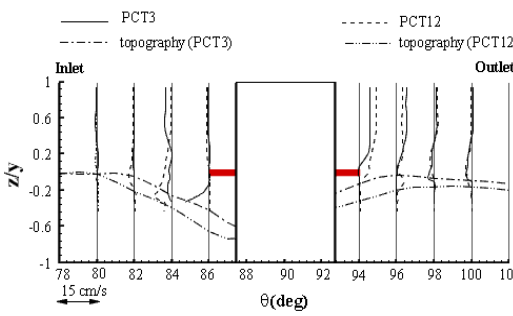
In Fig. 14(c), above the protected pier the vertical velocity due to the flow clash to the pier is negative and toward the bed. At an angle of 84 degrees, by increasing the collar thickness the vertical velocity gets negative and it increases the flow tendency toward the bed. At a distance of 4 times the pier diameter below the protected pier at a distance of 70% of the flow depth from the surface of the water, the vertical velocity value is positive and moves towards the flow surface. At 5%, the flow depth is reduced from the bed level of the vertical velocity and the flow moves to the bed. Also, it can be seen that at an angle of 98 and 100 degrees of bend, the increase in the collar thickness does not have a significant effect on vertical velocity, and the process of changes is approximately the same.



(a)



(b)



(c)

**Fig. 14. A sample of velocity distribution a) tangential, b) radial and c) vertical in the longitudinal section of the bend.**

Figure 15, shows the Reynolds stresses at 1 cm level above initial bed level are equal to 5% of the flow depth at the initial bed level. The Reynolds shear stress is calculated from the following equation (Das *et al.*, 2013b):

$$\tau_{yx} = -\rho \overline{u'v'} \quad (1)$$

$$\tau_{zx} = -\rho \overline{u'w'} \quad (2)$$

$$\tau_{zy} = -\rho \overline{v'w'} \quad (3)$$

In the relations (1), (2) and (3)  $\tau_{yx}$  is the shear stress on the y plate in the direction x,  $\tau_{zx}$  is the shear stress on the z-plate in the direction x and  $\tau_{zy}$  of the shear stress in the z-plate and in the y-direction. Also,  $u'$ ,  $v'$  and  $w'$  are frequent velocities and  $\rho$  is the water density. The method of calculating the product of frequent velocity in three directions is given in the following equations (Das *et al.*, 2013b).

$$\overline{u'v'} = \frac{1}{n} \sum_{i=1}^n (u - \bar{u})(v - \bar{v}) \quad (4)$$

$$\overline{u'w'} = \frac{1}{n} \sum_{i=1}^n (u - \bar{u})(w - \bar{w}) \quad (5)$$

$$\overline{v'w'} = \frac{1}{n} \sum_{i=1}^n (v - \bar{v})(w - \bar{w}) \quad (6)$$

In Eqs. (4), (5) and (6),  $\bar{u}$ ,  $\bar{v}$  and  $\bar{w}$  are respectively the average flow velocities in the longitudinal, transverse and deep directions.

In Fig. 15(a), in the PCT3 test, the maximum Reynolds stresses  $\tau_{yx}$  occurred at the above pier of the protected pier at an angle of 82 degrees. By increasing the collar thickness (PCT12), this stress is near zero. As the collar thickness increases, the Reynolds stresses  $\tau_{yx}$  decreases around the pier. This can be due to an increase in the dimensions of the scour hole around the thicker protected pier.

In Fig. 15(b), the Reynolds stresses  $\tau_{zx}$  in the first half of the bend are almost close in both tests, but by getting close to the protected pier, the values of this stress are completely different in the two tests. In addition, the rate of Reynolds stresses  $\tau_{zx}$  in the PCT3 test is increased in the range of 65 to 100 degrees compared to the beginning of the bend, and with increasing the collar thickness of this Reynolds stresses in the range is significantly reduced. Also in the second half of the bend maximum  $\tau_{zx}$  occurred in both tests near the inner bank, the amount of which in the PCT3 test was equal to 165gr /cm.s<sup>2</sup>, and decreased by 40% with the increase of the collar thickness.

Figure 15(c) shows the Reynolds stress  $\tau_{zy}$ . As can be seen, in the first and second half of the bend, increasing the collar thickness does not change much for this stress. In the PCT3 test, the highest stress  $\tau_{zy}$  occurred at above the pier and at an angle of 82 degrees, which is about 20 gr/cm.s<sup>2</sup>, with a decrease in the collar thickness the amount is

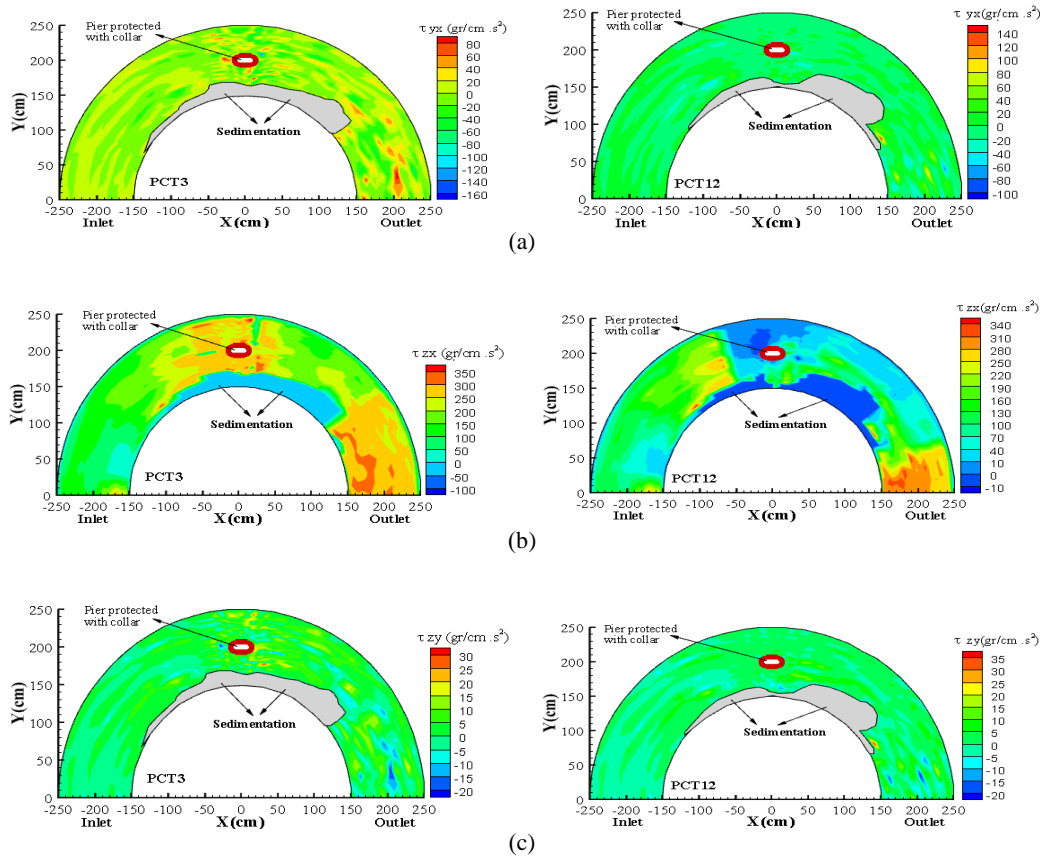


**Fig. 15.** Distribution of Reynolds shear stresses at a level of 5% of the flow depth at the beginning of the bend from the initial bed level a)  $\tau_{yx}$  b)  $\tau_{zx}$  and c)  $\tau_{zy}$ .

decreased to 2 gr/cm.s<sup>2</sup>. In general, in the area around the pier by increasing the collar thickness the  $\tau_{zy}$  stress decrease.

To investigate the effect of increasing the collar thickness on the amount of turbulent kinetic energy, the maximum kinetic energy per unit mass flow for both tests is presented in Fig. 16. Equation (7) is used to calculate kinetic energy due to velocity or turbulence fluctuations (Das *et al.*, 2013b).

$$TKE = \frac{1}{2}(\overline{u'^2} + \overline{v'^2} + \overline{w'^2}) \quad (7)$$

In the first half of the bend, the trend of kinetic energy variation on the unit of mass in both tests is almost close to each other.

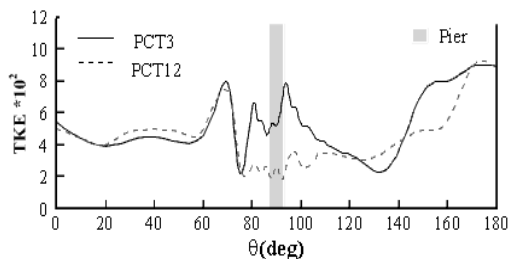


**Fig. 16.** Maximum kinetic energy values along the bend.

By approaching to the pier location, the maximum changes in kinetic energy per unit mass in each test is different. In a way that the maximum kinetic energy at the angle of 80 ° for the PCT3 test is 620 cm<sup>2</sup>/s<sup>2</sup>.gr, which decreases with a 60% increase in collar thickness. The minimum kinetic energy peak in PCT3 and PCT12 tests are occurred at 75 degrees and 92 degrees, respectively. In the PCT3 test, at the bottom of the pier in the range of 95 to 130 degrees, the maximum graph decreases the kinetic energy and by approaching to the end of the bend, the magnitude of the maximum kinetic energy increases. In addition, the maximum kinetic energy occurred in two tests at an angle of 180 degrees, which is approximately equal to 900 cm<sup>2</sup>/s<sup>2</sup>.gr.

#### 4. CONCLUSION

By examining the flow pattern around the pier protected with collar, it is observed that as the flow collides with the pier, the streamlines are separated from each other that, their direction in the outer half of the bend is toward the outer bank and in the inner side of the bend is toward the inner bank. Also, by increasing the thickness of the collar, the deviation of streamlines at the pier upstream will also increase as the collar collides the bed bottom. With the deviation of the streamlines due to the increased collar thickness towards the bed bottom, the maximum scour hole depth increased by 30%. Also,

by examining the streamlines in the plan associated with the level of 5% from the flow depth at the beginning of the bend above the initial bed surface it is observed that, the streamlines separated from each other due to collision with the collar pier in the PCT3 test from the pier tail 12 times the pier diameter which increased by 60%, with an increase in the collar thickness. Approaching the flow surface, the connection location of the streamlines separated has been approximately equal, and the collar thickness does not have a significant effect, and occurs near the pier tail.

## REFERENCES

- Abdi Chooplou, Ch. and M. Vaghefi (2019). Experimental Study of the Effect of Displacement of Vanes Submerged at Channel Width on Distribution of Velocity and Shear Stress in a 180 Degree Bend. *Journal of Applied Fluid Mechanics* 12(5), 1417-1428.
- Abdi Chooplou, Ch., M. Vaghefi and S. H. Meraji (2018). Study of Streamlines under the Influence of Displacement of Submerged Vanes in Channel Width, and at the Upstream Area of a Cylindrical Bridge Pier in a 180 Degree Sharp Bend. *Journal of Hydraulic Structures* 4(1), 55-74.
- Ataie-Ashtiani, B. and A. Aslani-Kordkandi (2012). Flow field around side-by-side piers with and without a scour hole. *European Journal of Mechanics B/Fluids*, 36, 152-166.
- Ataie-Ashtiani, B. and A. Aslani-Kordkandi (2013). Flow Field around Single and Tandem Piers. *Flow Turbulence and Combustion* 90(3), 472-490.
- Barbhuiya, A. K. and S. Talukdar (2010). Scour and three dimensional turbulent flow fields measured by ADV at a 90 horizontal forced bend in a rectangular channel. *Flow measurement and Instrumentation* 21(3), 312-321.
- Beheshti, A. A. and B. Ataie-Ashtiani (2010). Experimental Study of Three Dimensional Flow Field around a Complex Bridge Pier. *Journal of engineering mechanics ASCE* 136(2), 143-154.
- Beheshti, A. A. and B. Ataie-Ashtiani (2016). Scour hole influence on turbulent flow field around complex bridge piers. *Flow. Turbulence and Combustion* 97(2), 451-474.
- Belcher, B. J. and J. F. Fox. (2009). Laboratory measurements of 3-D flow patterns and turbulence in straight open channel with rough bed. *Journal of Hydraulic Research* 47(5), 685-688.
- Ben Mohammad Khajeh, Sh., M. Vaghefi and A. Mahmoudi (2017). The scour pattern around an inclined cylindrical pier in a sharp 180-degree bend: an experimental study. *International Journal of River Basin Management* 15(2), 207-218.
- Constantinescu, G., S. Miyawaki, B. Rhoads, A. Sukhodolov and G. Kirkil (2011). Structure of turbulent flow at a river confluence with momentum and velocity ratios close to 1: Insight provided by an eddy-resolving numerical simulation. *Water Resources Research* 47(5), 5507.
- Das, S. and A. Mazumdar (2015). Turbulence flow field around two eccentric circular piers in scour hole. *International Journal of River Basin Management* 13(3), 343-361.
- Das, S., R. Das and A. Mazumdar (2013a). Circulation characteristics of horseshoe vortex in scour region around circular piers. *Water Science and Engineering* 6(1), 69-77.
- Das, S., R. Das and A. Mazumdar (2013b). Comparison of characteristics of horseshoe vortex at circular and square piers. *Research Journal of Applied Sciences, Engineering and Technology* 5(17), 4373-4387.
- Dey, L., A. K. Barbhuiya and P. Biswas (2017). Experimental study on bank erosion and protection using submerged vane placed at an optimum angle in a 180° laboratory channel bend. *Geomorphology* 283, 32-40.
- Dey, S. and R. V. Raikar (2007). Characteristics of horseshoe vortex in developing scour holes at piers. *Journal of Hydraulic Engineering ASCE* 133(4), 399-413.
- Gholami, A., H. Bonakdari, A. A. Akhtari and I. Ebtehaj (2019). A combination of computational fluid dynamics, artificial neural network and support vectors machines model to predict flow variables in curved channel. *Scientia Iranica* 26(2), 726-741.
- Karimi, N., M. Heidarnajad and A. Masjedi (2017). Scour depth at inclined bridge piers along a straight path: A laboratory study. *Engineering Science and Technology, an International Journal* 20(4), 1302-1307.
- Khan, M., M. Tufail, M. Ajmal, Z. U. Haq and T. W. Kim (2017). Experimental analysis of the scour pattern modeling of scour depth around bridge piers. *Arabian Journal for Science and Engineering* 42(9), 4111-4130.
- Kirkil, G. and G. Constantinescu (2010). Flow and turbulence structure around an in-stream rectangular cylinder with scour hole. *Water Resources Research* 46(11), W11549.
- Kirkil, G., S. G. Constantinescu and R. Ettema (2008). Coherent structures in the flow field around a circular cylinder with scour hole. *Journal of Hydraulic Engineering ASCE* 134(5), 572-587.
- Kumar, U. C., K. G. Kothiyari and R. Ranga (2012). Flow structure and scour around circular component bridge piers - A review. *Journal of Hydro-environment Research* 6(4), 261-265.

- Leschziner, M. A. and W. Rodi (1979). Calculation of strongly curved open channel flow. *Journal of the Hydraulics Division* 105(10), 1297-1314.
- Ma, M., J. Lu and G. Tryggvason (2015). Using statistical learning to close two-fluid multiphase flow equations for a simple bubbly system. *Physics of Fluids* 27(9), 092101.
- Ma, M., J. Lu and G. Tryggvason (2016). Using statistical learning to close two-fluid multiphase flow equations for bubbly flows in vertical channels. *International Journal of Multiphase Flow* 85, 336-347.
- Melville, B. W. and A. J. Sutherland (1988). Design method for local scour at bridge piers. American Society of Civil Engineering. *Journal of the Hydraulics Division* 114(10), 1210-1225.
- Naji Abhari, M., M. Ghodsian, M. Vaghefi and N. Panahpur (2010). Experimental and numerical simulation of flow in a 90 degree bend Flow. *Measurement and Instrumentation* 21(3), 292-298.
- Oliveto, G. and W. H. Hager (2002). Temporal evolution of clear-water pier and abutment scour. *Journal of Hydraulic Engineering* 128(9), 811-820.
- Rodríguez, J. F. and M. H. García (2008). Laboratory measurements of 3-D flow patterns and turbulence in straight open channel with rough bed. *Journal of Hydraulic Research* 46(4), 465-454.
- Şarlak, N., and Ş. Tiğrek (2011). Analysis of experimental data sets for local scour depth around bridge abutments using artificial neural networks. *Water Sa* 37(4), 595-602.
- Tang, X. and D. W. Knight (2014). The lateral distribution of depth-averaged velocity in a channel flow bend. *Journal of Hydro-environment Research* 10, 1-10.
- Tryggvason, G., M. Ma and J. Lu (2016). DNS-Assisted modeling of bubbly flows in vertical channels. *Nuclear Science and Engineering* 184(3), 312-320.
- Uddin, M. N. and M. M. Rahman (2012). Flow and erosion at a bend in the braided Jamuna River. *International Journal of Sediment Research* 27(4), 498-509.
- Vaghefi, M., M. Akbari and A. R. Fiouz (2015). Experimental Study of Turbulence Kinetic Energy and Velocity Fluctuation Distributions in a 180 Degree Sharp Bend. *10th International Congress on Civil Engineering*, University of Tabriz, Tabriz, Iran.
- Vaghefi, M., M. Akbari and A. R. Fiouz (2016). An experimental study of mean and turbulent flow in a 180 degree sharp open channel bend: Secondary flow and bed shear stress. *KSCE Journal of Civil Engineering* 20(4), 1582-1593.
- Vaghefi, M., M. Moghanloo, D. Dehghan and A. Keshavarz (2017). Experimental Study of the Effect of Base-level fall at the Beginning of the Bend on Reduction of Scour around a Rectangular Bridge Pier Located in the 180 Degree Sharp Bend. *Journal of Hydraulic Structures* 3(2), 32-46.
- Zarrati, A. R., H. Gholami and M. B. Mashahir (2004). Application of collar to control scouring around rectangular bridge piers. *Journal of Hydraulic Research* 42(1), 97-103.